



Destekli Akım Alan Sargılı 18-12 Çıkık Kutup Yapılı Fırçasız dc Motor: Tasarım Manyetik Alan Üzerine Tasarım Optimizasyonu ve Nümerik Analiz

Hassan Moradi CheshmehBeigi*

Electrical Engineering Department, Faculty of Engineering, Razi University, Kermanshah 67149, Iran

Received: 22.07.2015; Accepted: 10.09.2015

Özet. Bu çalışma 3 boyutlu sonlu element analizi kullanarak bir 18-12 aşamasındaki Brushless dc motorun (BLDCM) dizayn optimizasyonu ve tam elektromanyetik alan analizini sunmaktadır. Sunulan motor rotor yapısında kalıcı mıknatıs ile değiştirilen dc ile desteklenen alan sargısı tarafından kontrol edilen geniş çaplı bir hava boşluğu akışı sağlayacaktır. Sunulan basit bir dc akım kontrolü BLDCM kullanılmıştır ve bu kontrolü sunmak için hiçbir fırça veya slip halkaya ihtiyaç duyulmamıştır. İstenilen performans belirli bir kapalı alanda ulaşmak için sunulan düzenlemenin fiziksel boyutları ortalama güç üretimini maksimize yapacak şekilde optimize edilmiştir. Sunulan 18-12 BLDCM konfigürasyonu bir 9-6 konfigürasyonu ile karşılaştırılmıştır. Motor performansını hesaplamak için sayısal tekniklerden yararlanılmıştır. Sayısal bölümde, 3-D sonlu eleman (FE) analizi iki tip BLDCM için sunulan dizayn işleminin doğruluğunu ve verimliliğini onaylamak amacıyla bir manyetik CAD paketi (Infolytica Corporation Ltd.) kullanılarak yapılmıştır. Analiz sonuçları sunulan makine dizayn metodolojisinin verimliliğini kanıtlamaktadır.

Anahtar Kelimeler: FE Analiz; Alan analizi; Fırçasız Dc Motor

18-12 Salient-Pole Structure Brushless dc Motor with an Assisted dc Field Coil: Design Optimization and Numerical Analysis on the Magnetic Field

Abstract. This paper presents the design optimization and accurate electromagnetic field analysis of an 18-12 three phase Brushless dc motor (BLDCM) by using a three-dimensional Finite-Element analysis. Proposed motor will provide a wide range of air-gap flux control by a dc assisted field winding which is replaced with the permanent magnet in the rotor structure. In proposed BLDCM a simple dc current control is used and no brushes or slip rings are required to perform this control. To achieve the required performance within a specified space envelope, the physical dimensions of the proposed configuration were optimized; subject to maximize the average output power. Proposed 18-12 BLDCM configuration has been compared with a 9-6 BLDCM configuration. To evaluate the motor performance, the numerical techniques have been utilized. In the numerical part, 3-D Finite Element (FE) analysis has been carried out using a MagNet CAD package (Infolytica Corporation Ltd.) for two type of BLDCM to confirm the accuracy and the efficacy of the proposed design procedure. The analysis results demonstrate the effectiveness of the proposed machine design methodology.

Keywords: FE Analysis; Field analysis; Brushless Dc Motor

1. INTRODUCTION

The brushless dc motor (BLDC) is one of the challenges for simple construction, high reliability and high power density in variable speed drive applications such as automotive, Aerospace, home appliances, and many industrial equipments and instrumentations [1- 4]. However, because of the uncontrollable permanent-magnet (PM) flux, it suffers from a short

*Corresponding author. Email: Ha.moradi@razi.ac.ir

constant-power operating range. The permanent-magnet utilized in BLDC motor has several intrinsic disadvantages such as; increased motor cost, Limited operating-speed range, Demagnetization of the permanent magnet [5-7].

These problems have been addressed by many researchers [8-11]. To improve the motioned problems of conventional PMLBDC this paper presents a new three phase BLDC motor configuration in which in the rotor permanent magnet is replaced by an assisted field. The dc current in the assisted field coil produces an axial magnetic flux which makes the on rotor assembly magnetically north and the other one as south magnetically. Therefore, the magnitude of generated magnetic field can be controlled by controlling the field current. The absence of rotary windings and permanent magnets on the rotor support both high rotational speeds and high-temperature operation. It should be mentioned that, the presented motor can generate both the magnetic torque which is approximately proportional to the field current which offers the characteristics of a brushed dc series machine, and the reluctance torque which is approximately proportional to the phase current, offering the characteristics of a SR machine. Using assisted field replaced with permanent magnet in the rotor and generating the magnetic and reluctance torques are main significant characteristics of proposed motor which highlights this family of BLDC motor in comparison with the conventional BLDC motors.

Complex geometry and nonlinear properties of the proposed Salient-Pole structure is the main reason for calculation and analysis of the flux distribution inside the machine for different excitation currents and rotor positions. So, an accurate knowledge of the magnetization characteristics is essential for the prediction and evaluation of machine performance. Numerical analysis methods such as FE technique gives precise information of the machine parameters such as, magnetic flux density, inductances and electromagnetic torques based on magnetic field calculation using machine geometry, dimensions, and materials. FE analysis is capable of considering the magnetic field saturation effect based on machine performance. Presented BLDC motor, owing to its special construction necessitates 3-D finite-element analysis for accurately calculating its performance such as developed torque, etc. It provides not only confirmations of the investigation of the results but also the exact illustration of magnetic field distribution for this motor with complex geometry.

This paper presents and analyzed an 18/12 BLDC motor in which permanent magnet is replaced with assisted field coil in the rotor. The field coil can be energized by dc current. This paper is managed the following manner. Section II describes the BLDC structure and

operation. Section III describes design procedure, and section IV describes optimization, Section V describes FEM analysis. Finally, conclusion is presented.

2. STRUCTURE OF THE MOTOR

Structure and 3-D view of the proposed three phases BLDC motor are shown in Fig. 1 and basic dimensions and specifications are also shown in Table I. The motor shown in Fig.1 has steel laminations on the rotor and stator. The stator and rotor are constructed with two dependent magnetically sets, in which the two sets are exactly symmetrical with respect to a plane perpendicular to the middle of the motor shaft.

- Each layer consists of 18 stator poles with phase winding coils and 12 rotor poles, respectively.
- The coils around each individual pole are connected to form the phase windings. This is a three phase machine, therefore, three coil windings from one layer is connected in series with the other three coil windings in the other layer.
- There is a stationary reel which is a rotating cylindrical core, which has the assisted field coil, wrapped around it and is placed between the two-stator sets.

Motor dimensions such as stator and rotor pole arcs, air-gap length, and diameter of the shaft are shown in Table I. It should be noted that, the design of the pole arcs should satisfy the basic requirements for self-starting, higher torque output, and lower torque ripple. Fig.2 shows a structure and a field flux path of proposed configuration. The magnetic flux produced by the coils travels through the guide and shaft to the rotor and then to the stator poles, and finally closes itself through the motor housing (Fig. 2). It is worth mentioning that, the number of stator poles and their configuration is completely different than that of the switched reluctance motor.

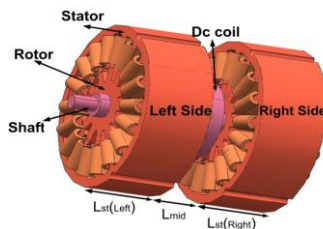


Fig.1 - 3-D view of the motor

The suggested configuration is to some extent similar to the Switched Reluctance (SR) machine, but it is worth mentioning that, the number of stator and rotor poles and their configuration, phases overlap region, number of phases that can be excited simultaneously and commutator to excite the phases is completely different than that of the SR motor.

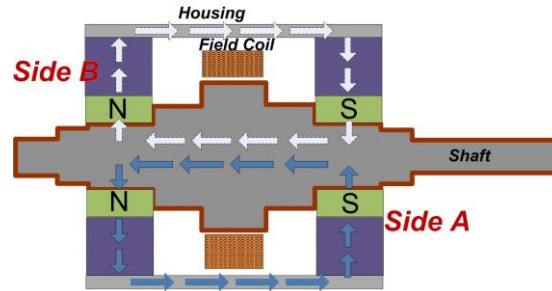


Fig.2 - 3-D view of flux path

Table 1. Geometric parameters of proposed configuration

P_{out}	Watt	1500
V_{in}	Volt	24
Speed	rpm	3500
I_p	Amp.	74
D_r	mm	66
D_s	mm	140
$L_{stk.}$	mm	94
N_s	-	18
N_r	-	12
β_s	Deg	14
B_r	Deg	14
L_g	mm	0.3
h_s	mm	29
h_r	mm	12
T_{ph}	Turns	50
D_{sh}	mm	20

Principle of operation

The major parameters and the design features of the proposed three phase BLDC motor are shown in Fig. 1 and basic dimensions and specifications are shown in Table I. The stator and rotor are constructed with two dependent magnetically sets. Each stator set has 18 teeth with phase winding coils. One possible layout for the windings is shown in Fig. 3. Also, each rotor set has 12 teeth. In this geometry, an assisted field replaced with permanent magnet in the rotor, the field winding carries dc current and is permanently energized. The dc current in the field winding gives axial flux along the length of the rotor; this means that, at one end flux is leaving the rotor while at the other it is entering. Consequently, making the rotor magnetically polarized at its ends. As mentioned before, each stator set comprises nine teeth, and there are concentrated windings placed around each salient pole. This is a three phase salient pole machine, therefore, three coil windings from one layer is connected in series with the other three coil windings in the other layer. Consequently, when each phase is energized the magnetic flux that is produced at each stator pole is in the same direction as the required flux path (The magnetic field flows axially through the rotor shaft and closes through the stator teeth and the machine housing). When a phase is energized, stator poles of side A become a south pole and the other side (side B) becomes a north pole (Fig. 2). Besides, assisted field winding, depending on its current direction, polarizes the rotor so one end is an effective south pole and the other an effective north pole, then the like poles will repel and the unlike poles attract which gives the torque to turn the machine. Complex structure and intrinsic nonlinear properties of the magnetic materials of the presented novel BLDC machine, is main reason for calculation and analysis of the flux distribution inside the machine.

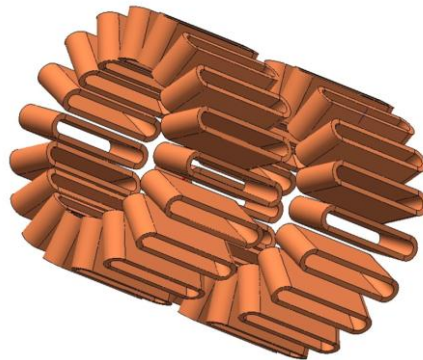


Fig.3 Concentrated 3-phases winding for proposed motor.

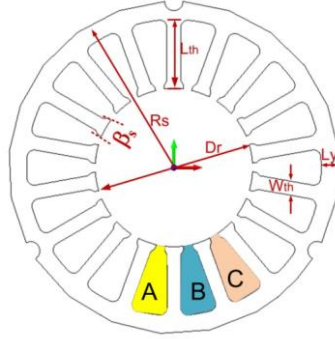


Fig. 4 Geometry parameters

3. ELECTROMAGNETIC DESIGN:

In order to obtain adequate dimensions for the prototype to be built a set of equations are derived to relate mechanical dimensions, electromagnetic restrictions, and technical constraints. Finally, an optimization based on surface current density and minimum total volume of the machine is carried out to obtain optimum geometry (Fig. 4).

If excitation current of the field winding is injected, with a positive or negative polarity, flux of the iron pole section will change linearly if the iron saturation is neglected.

$$\varphi_g = \mu_0 \frac{N_f I_f}{l_g A_g} \quad (1)$$

$$\varphi_{ts} = \varphi_g / N_r = \varphi_g / 12 \quad (2)$$

$$\lambda_{max} = N_{ph} \times \varphi_{ts} \quad (3)$$

φ_g	Air-gap flux,
N_f	The number of turns of field winding,
N_{ph}	The number of turns of phase winding,
I_f	Field current,
l_g	Air-gap length,
φ_{ts}	The stator teeth flux,
N_r	The number of rotor teeth,

Consider the flux linkage λ of one coil with “ N_f ” turns as the rotor rotates.

18-12 Salient-Pole structure Brushless dc Motor with an assisted dc Field coil

The preliminary selection of frame size automatically fixes the outer diameter of the stator. It should be mentioned that, the Frame Size is given according to the IEC recommendations. Practically, the outer diameter of the stator is fixed as follows:

$$D_0 = (\text{Frame Size} - 3) \times 2 \quad (4)$$

During the progression of the design, if the machine size is found to be too large or too small, a different frame size can be used. The ratio of the rotor diameter to the rotor length can be assumed between 0.65~0.95. According to this ratio the rotor size can be roughly estimated by the:

$$P = \pi^2 \times D_r^2 \times L_{st} \times 10^3 \times \omega \quad (5)$$

where D_r is rotor diameter, L_{st} is rotor length. Next, decide on the air gap.

Assuming that the stator pole flux density B_s ($B_s = 1.6 \text{ Tesla}$) is assumed to be equal to B_{max} the rest of the machine can be designed. Neglecting leakage and stacking factor, the stator pole area A_s can be written as:

$$A_s = \left(\frac{D_r}{2} + l_g \right) \times L_{st} \times \beta_s \quad (6)$$

where l_g is air gap length and β_s is stator pole arc. The flux in the stator pole is given by: $\Phi_{ts} = B_s \times A_s$. Specific magnetic loading can be written as:

$$B_{av} = \left(2 \times \frac{\frac{N_s \times \Phi_{ts}}{N_{ph}}}{\pi \times D_r \times L_{st}} \right) \quad (7)$$

and Specific electric loading is:

$$ac = \frac{P_a}{\pi D_r^2 \times L_{st} \times B_{av} \times n} \quad (8)$$

The total number of conductors is defined by Z , for a three-phase machine it can be obtained by,

$$Z = \frac{ac \times \pi \times D_r}{l_z} \quad (9)$$

and T_{ph} can be obtained by:

$$T_{ph} = \frac{Z}{\frac{N_s}{N_{ph}} \times 2} \quad (10)$$

The area of stator slot is found with a certain slot height (h_s) selected:

$$A_{slot} = \frac{\pi}{Q} \left[\left(\frac{D_{is}}{2} + h_s \right)^2 - \left(\frac{D_{is}}{2} \right)^2 \right] - b_{ts} h_s \quad (11)$$

The major parameters and the design features of the proposed three phase generator are shown in Fig.4 and basic dimensions and specifications are shown in Table 1.

Three Dimensional Fem Analyses

By applying machine geometry dimensions and materials, magnetic field calculation for the machine parameters such as magnetic flux density, inductances and electromagnetic torques done precisely with FE techniques. FEM has the ability to take into account the effects of magnetic field saturation based on machine performance. Only symmetrical side of the machine to the field coil is considered in 3-D analysis. The field analysis has been performed using a Magnet CAD package (Infolytica Corporation Ltd., 2007), which is based on the variational energy minimization technique to determine the magnetic vector potential [16]. In this paper, the variational energy minimization technique, known as T- Ω formulation, is employed for solving magnetic field problems [15-16].

$$\nabla \cdot \mathbf{T} - \nabla \cdot (\nabla \Omega) = 0 \quad (10)$$

$$\begin{cases} \nabla^2 \mathbf{T} - \mu \sigma \left(\frac{\partial \mathbf{T}}{\partial t} \right) = -\mu \sigma \nabla \left(\frac{\partial \Omega}{\partial t} \right) \\ \nabla^2 \Omega = 0 \end{cases} \quad (11)$$

18-12 Salient-Pole structure Brushless dc Motor with an assisted dc Field coil

T Electric vector potential,

Ω Magnetic scalar potential,

T and Ω Are defined by $\mathbf{j} = \nabla \times \mathbf{T}$ and $\mathbf{H} = \mathbf{T} - \nabla\Omega$

To solve the problem with 3-D analysis, the computed quantities were assumed to remain constant when considering different sections of the machine; also the materials of which the machine is made are considered to be isotropic. Regarding the ferromagnetic material characteristics of the BLDC generator, to obtain a reliable FEM model, it is essential to specify its B–H curve. In the 3-D FE analysis, the cylindrical stator and rotor domains were meshed using eight-node quadrilateral and six-node triangular finite elements. Dense meshes are set to points where the field fluctuations are significant. By utilizing a MagNet CAD package (Infolytica Corporation Ltd., 2007), which applies the finite element technique for a fast and precise solution of Maxwell's equations, the field analysis has been calculated.

4. DESIGN OPTIMIZATION

An FEM analysis optimization routine for the optimum design of a proposed motor has been set up, which includes six FE analyses: three EM FEA for the different rotor position from the aligned to unaligned positions to find the optimum rotor pole geometry, three EM FEA for the air gap length to find the maximum flux linkage, The electromagnetic FEA and design optimization searches were implemented in a commercial Magnet CAD package (Infolytica Corporation Ltd., 2007).

Air Gap Length

Fig. 5 presents the flux Linkage of the understudy generator for different air gap values. It clearly shows the influence on the maximum flux Linkage as well as the flat flux Linkage range on the characteristics. Hence the machine with the smallest air gap length, subject to acceptable manufacturing tolerances, will produce the highest average flux linkage. However, the original air gap length of $g=0.2\text{mm}$ and therefore the rotor outer diameter remain unchanged due to manufacturing tolerances.

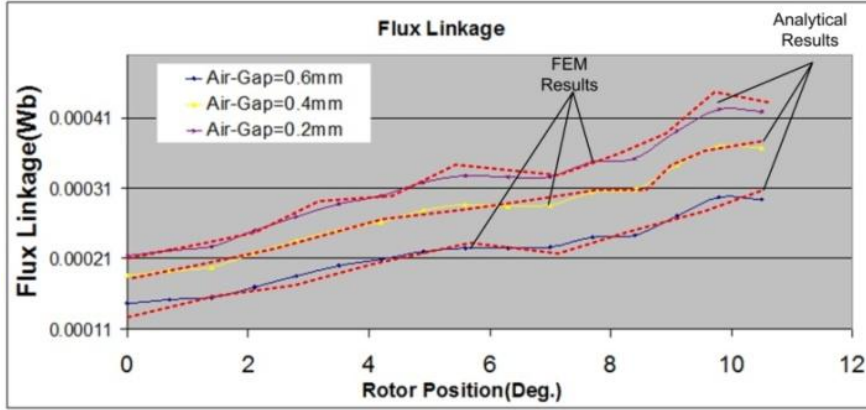


Fig.5 flux Linkage of the understudy generator for different air gap values

Optimization Rotor Pole Geometry:

The rotor outer diameter was chosen with the goal to produce a maximum output power. With respect to the previous calculations of the stator geometry it is $D_r=66$ mm. In order to find the optimum rotor pole geometry, parallel shaped poles are assumed. The shaft diameter is fixed with $D_{sh}=20$ mm. The influence of constructional rotor parameter on maximum output power was investigated. These parameter were changed in the range of rotor pole height $h_r=[10,11,12,13,14]$ mm and rotor pole width $\beta_r=[12,13,14,15,16,17]$ Deg. Analytical calculations have been made as well as FEM calculations for comparison and to verify the different machine models. The Field coil is assumed to be excited by $mmf=100$ Amp-turns.

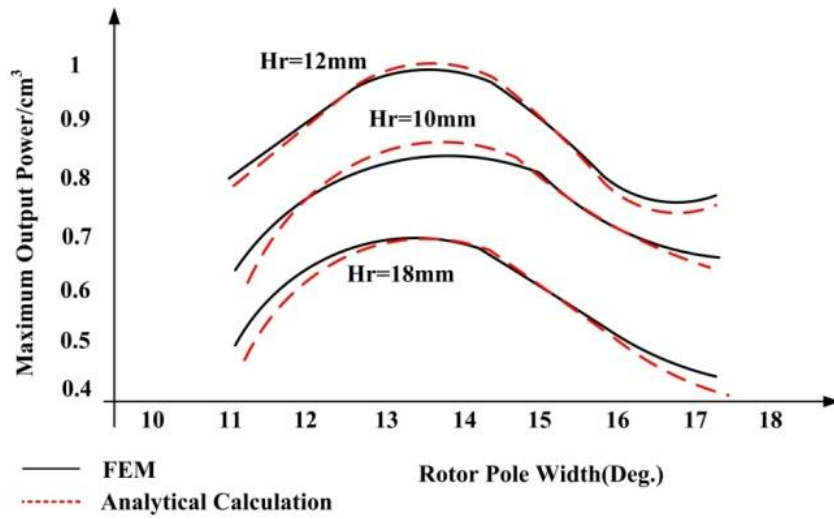


Fig.6 The influence of constructional rotor parameter on maximum output power

Referring to Fig. 6 it is found that the optimum rotor pole parameters are $\beta_r=14\text{mm}$ and $h_r=12\text{mm}$. Note the good agreement of the calculation results obtained by FEM and by analytical methods. The results for the presented configuration summarize Table 1 for the optimum geometric parameters.

5. FE ANALYSIS RESULTS AND DISCUSSION

In this study, a 3-D FE analysis with apply normal field boundary conditions over the inner and outer borders of the machine is being used to determine the magnetic field distribution in and around the motor. In order to present the operation of the motor and to determine the static torque at different positions of the rotor, the field solutions are obtained. As mentioned before, Magnet CAD package [13], has been used to solve nonlinear Poisson's equations and therefore to obtain the magnetic vector potential of each node element in the proposed configuration. Design the geometrical model, allocate physical material properties, set up boundary conditions over the inner and outer borders of the machine and considering an air box around the motor are essential steps for pre-processing stage of FEM analysis.

The cylindrical stator and rotor domains were meshed using six-node triangular finite elements (Fig. 7).

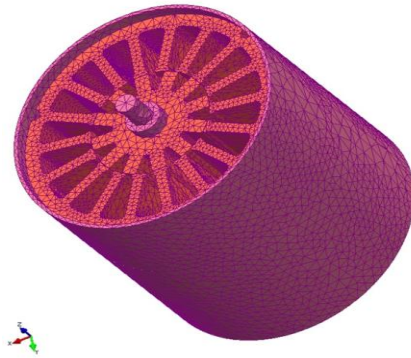


Fig.7 3-D Finite element meshes of a presented configuration.

In this study, the motor geometry has been analyzed, for different rotor angular position θ . This is defined as the angle between a certain pole stator (which is taken as reference) and one of the rotor poles. The angular positions considered between 0° and 30° in

1.5° increment steps. This covers the unaligned and aligned sequence between the machine poles.

The excitation currents are chosen to be in steps of 0.25 A from 0.25 A to 2 A. As mentioned before, the dc current in the field winding gives axial flux along the length of the rotor; this means that, at one end flux is leaving the rotor poles while at the other end the flux is entering the rotor pole. Fig. 8 shows distributed axial flux taken from 3-D FE Analysis along the length of the rotor assembly.

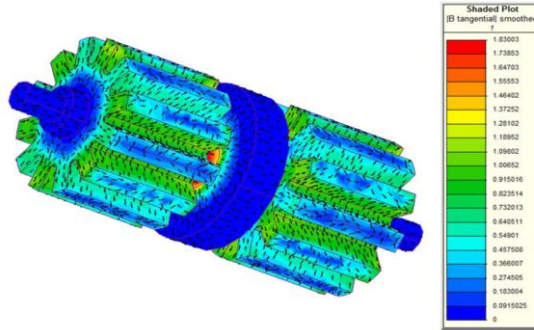


Fig.8 Distributed axial flux along the length of the rotor assembly

Furthermore, each stator set comprises 18 poles, and with concentrated windings placed around each salient pole. When each phase is energized the magnetic flux produced by each stator pole winding will travel in the same direction as the required flux path. Fig. 9 shows distributed flux at each stator pole for two dependent magnetically sets.

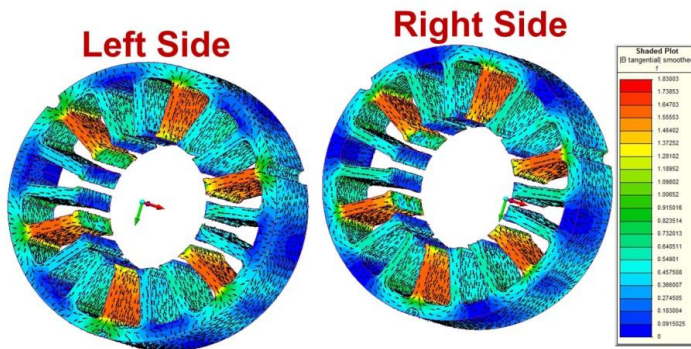


Fig.9 distributed flux at each stator pole for two dependent magnetically sets.

3-D FE analysis for different values of phase current's (I_{ph}) and field excitation current (0.1, 0.5, 0.75, 1 and 2 Amp.) have been analyzed. In this study two modes of excitation are considered. First, when the phase windings are considered to be turned on and

18-12 Salient-Pole structure Brushless dc Motor with an assisted dc Field coil

second, both the assisted field and the phase windings considered to be turned on. Flux distributions of the presented motor by utilizing 3-D FE analysis are shown in Fig. 10 when only the phase windings are considered to be turned on for a magnitude of $I_{ph} = 5$ A.

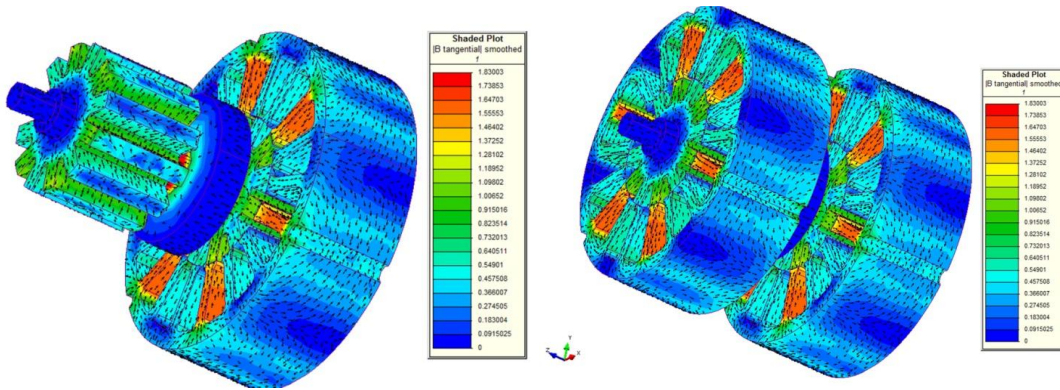


Fig.10 3-D View of distributed flux For $I_{ph}=5A$ and $I_{field}=0$ A.

Fig.11 show the Flux distributions when both, the field coil and the phases windings are excited, $I_{ph} = 5$ A and $I_{field} = .5$ A . It is worth mentioning here that, the stator and rotor cores are made of a non-oriented silicon steel lamination. The magnetization curve is taken from the manufacturer's data sheet for M-27 steel.

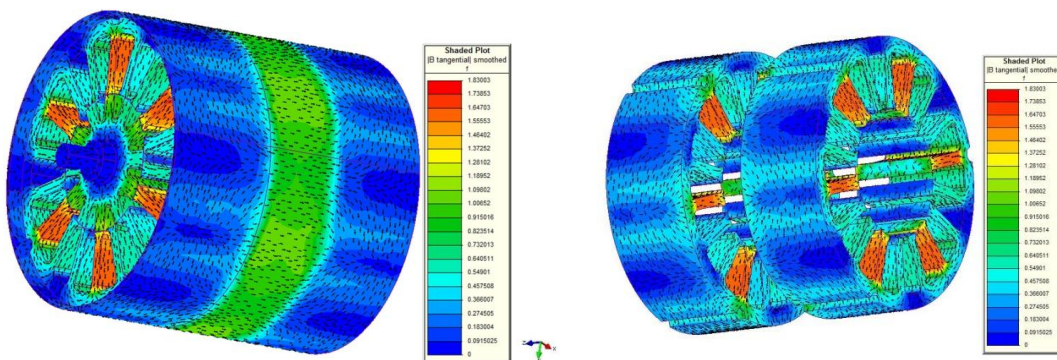


Fig.11 3-D View of distributed flux For $I_{ph}=5A$ and $I_{field}=0.5$ A.

As noted before, when an electrical current passed through the assisted field coil, an axial magnetic field is produced. The magnetic flux produced by the coil travels through the

guide and shaft to the rotor and then to the stator poles, and finally closes itself through the machine housing.

The magnitude of magnetic flux density in the stator poles with energized coil starts from 0.5 Tesla at the beginning of rotor/ stator pole un-alignment shown and increases to 1.26 Tesla for half alignment shown and then reaches to 1.53 Tesla at full alignment. The direction of magnetic flux travels from one energized stator pole winding to the yoke and then to the opposite stator pole as shown in Figs. 8-11.

The inductance has been defined as the ratio of each phase flux linkages to the exciting current (λ / I). Fig. 12 shows flux linkage for phase A and mutual flux for phases B,C when phase current (phase A) is 0.75A.

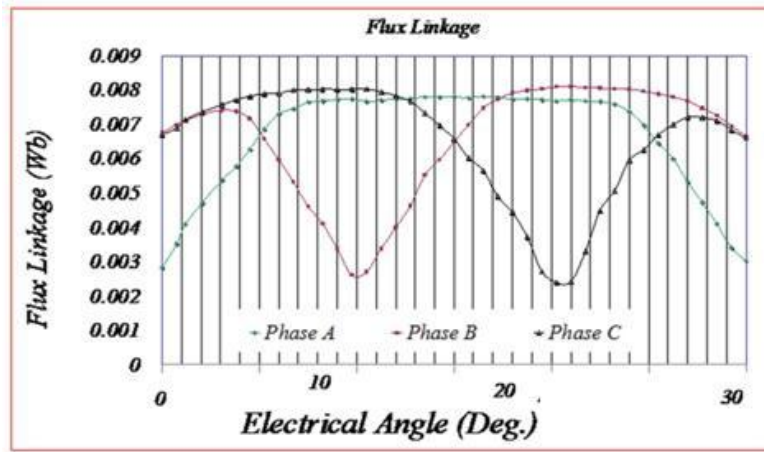


Fig.12 Flux linkage for phase A and mutual flux for phases B, C

The maximum inductance occurs at full alignment, when the field coil perceives two rotor pole sets which are positioned perpendicular to each other. Fig. 13 show the inductance profiles of the proposed **BLDC** at different I_{ph} and $I_{field} = 0$ A for various rotor positions. Here the maximum inductance value for the aligned position ($I_{ph} = 0.5$ A) obtained by using analytical method is 16 mH and minimum inductance value for the unaligned position is 6 mH. Fig. 14 shows the inductance profiles of the proposed **WPMBLDC** at different I_{ph} and $I_{field} = 0.5$ A for various rotor positions, consequently maximum and minimum inductance value for $I_{ph} = 0.5$ A is 12 mH and 4.5 mH respectively.

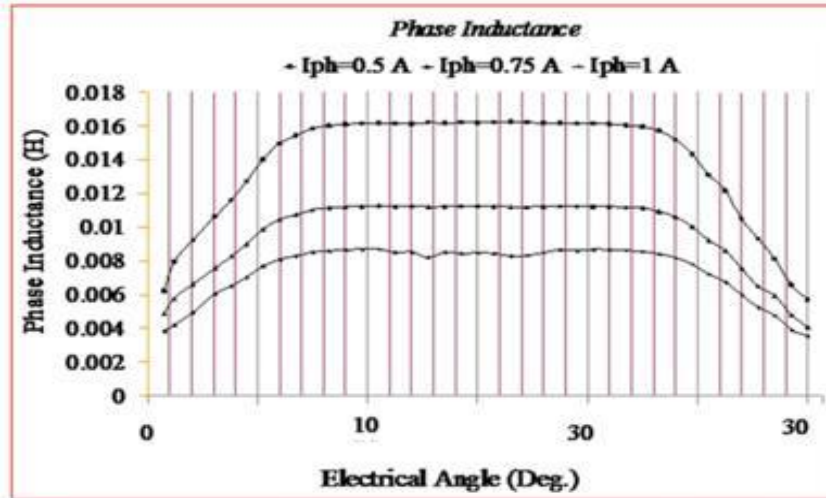


Fig.13 Inductance profiles at different I_{ph} and $I_{field} = 0\text{ A}$ for various rotor positions.

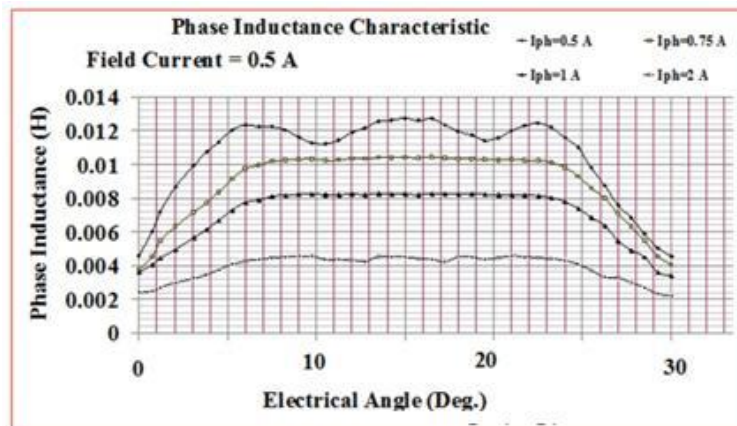


Fig.14 Inductance profiles at different I_{ph} and $I_{field} = 0.5\text{ A}$ for various rotor positions.

Structure of the 9-6 WPMBLDC Generator, Principle and operation:

The 9-6 WPMBLDC motor structure and some simulation and experimental results have been presented by authors [17]. In this configuration the basic dimensions are: a rotor pole arc of 30° , a stator pole arc of 30° and an air-gap length of 0.6 mm. For ease of manufacture, the diameter of the shaft is chosen to be 9 mm, the outer diameter of the rotor is 59.4 mm, and the length of the stator pole is 15 mm. Fig.15 illustrates the proposed 9/6 BLDC generator that is fabricated in the laboratory. It should be mentioned that principle and

operation of proposed 18-12 WPMBLDC Generator is same to presented 9-6 WPMBLDC Generator structure by reference [17].



Fig.15 Proposed BLDC generator fabricated in the laboratory

The output signals come from the photo-interrupters mounted on the back of the motor. There are three 30° pulses produced by the motor shaft position sensors and each pulse appears 6 times in one rotation. Fig. 16 shows the resulting pulses produced by the sensing unit for 30° duration. Fig. 17 shows the input current into the motor from the supply voltage.

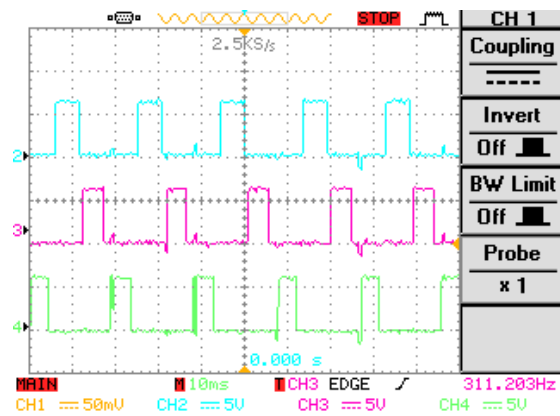


Fig.16 The output signals from the photo-interrupters

18-12 Salient-Pole structure Brushless dc Motor with an assisted dc Field coil

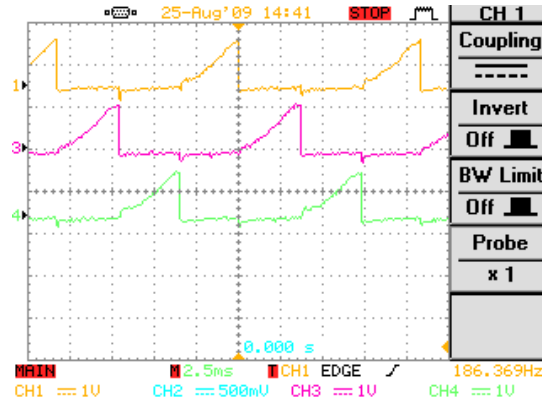


Fig.17 The input current into the motor from the supply voltage.

The torque-speed and torque-current characteristics of the motor for 3 different field currents are shown in Fig. 18. As shown in Fig. 18, the torque-speed characteristics of the motor behave like a series of DC motors and switched reluctance motor.

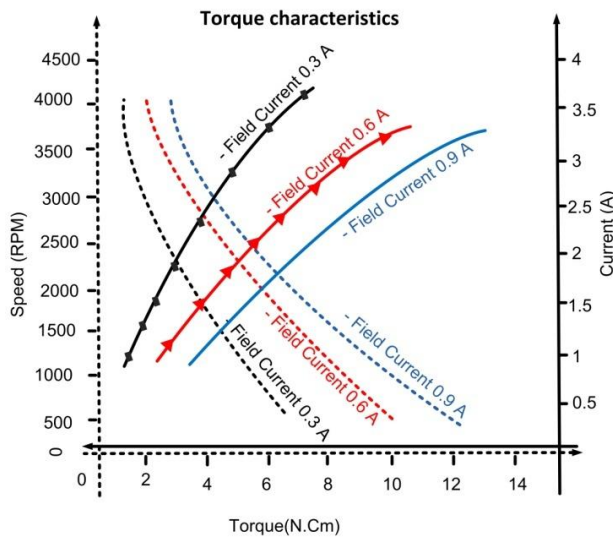


Fig.18 The motor torque characteristics

For the WPMBLDC machine, the absence of windings and permanent magnets on the rotor support both high rotational speeds and high-temperature operation. Furthermore, the absence of permanent magnets on the machine structure reduces the machine cost. Varying the amplitude and direction of the current in the field coil can control the output torque to a level between zero and the maximum. The nature of this configuration makes it compatible with any application that requires variable-speed operation.

Since the suggested configuration is to some extent similar to the Switched Reluctance (SR) motors, quantitative comparisons between the proposed motor and the SR motor can be explained as follow [17]:

1. Regarding the number of rotor poles for SR motors, when the poles of one phase come into full alignment, the poles of another phase are just starting to overlap and hence are available to seamlessly take over torque production. Even though , for the suggested motor, when one phase come into full alignment, 10° overlap for the poles of another phase is occurred.
2. Typical three-phase SR motors combinations for stator and rotor poles are 6/4, 8/6, 12/8, 18/12, etc. structures. Although for the proposed motor, the numbers of stator and rotor poles are 9/6.
3. For the SR motor, torque is produced by the tendency of its moveable part to move to a position where the inductance of the excited winding is maximized. But, in the presented structure, the torque is produced based on both the above feature for SR motors and the fundamental principle of magnetism which is used as basic operation of conventional BLDC motors. For the proposed motor, substitution of assistant field by permanent magnet in the rotor is carried out. When a current is passed through field coil, one set of rotor poles is magnetically north and the other set magnetically south. In addition to, when a current is passed through stator poles windings, it generates a magnetic field with N-S polarity on two sides of stator poles. As a consequence, by considering the influence of the opposite and similar poles on the stator and rotor, sufficient torque to move the rotor to a desired position can be achieved.
4. Due to proposed structure, two phases can be excited simultaneously. It provides higher power density in comparison with similar SR motors in which only one phase can be excited.
5. The magnetization pattern of the individual phases together with the $T-i-\theta$ characteristics of the salient poles motors dictate the amount of torque ripple during operation. Regarding to the designed configuration due to extension of overlap region, the torque ripple for the proposed motor is reduced in comparison with conventional SR motors.

Some advantages and disadvantages of proposed configuration are as follow:

18-12 Salient-Pole structure Brushless dc Motor with an assisted dc Field coil

- A wide range of air-gap flux control is obtained with a low field AT requirement. This control can be used to either reduce or increase the air-gap flux.
- The WPMBLDC motor magnetic configuration allows one to control the air-gap flux level without any demagnetization risk for the magnet pieces. Control action is performed over low-reluctance iron poles.
- A simple dc current control is used and no brushes or slip rings are required to perform this control.

However, the WPMBLDC motor presents some drawback due to its configuration.

- Additional dc winding reduces the power density. The required space reduces inner diameter and/or increases the outer diameter. In addition, air-gap surface associated to this winding does not participate in the energy conversion process.
- Three-dimensional (3-D) flux distribution introduces extra losses and increases material requirement. Stator and rotor core require tangential and axial flux conduction capacity. Additionally, there are some manufacturing problems.

6. CONCLUSION

This paper presents the design optimization and accurate electromagnetic field analysis of an 18-12 three phase Brushless dc motor (BLDCM) by using a three-dimensional Finite-Element analysis. Proposed motor will provide a wide range of air-gap flux control by a dc assisted field winding which is replaced with the permanent magnet in the rotor structure. In proposed BLDCM a simple dc current control is used and no brushes or slip rings are required to perform this control. To achieve the required performance within a specified space envelope, the physical dimensions of the proposed configuration were optimized; subject to maximize the average output power. Proposed 18-12 BLDCM configuration has been compared with a 9-6 BLDCM configuration. To evaluate the motor performance, the numerical techniques have been utilized. In the numerical part, 3-D Finite Element (FE) analysis has been carried out using a MagNet CAD package (Infolytica Corporation Ltd.) for two type of BLDCM to confirm the accuracy and the efficacy of the proposed design procedure. The analysis results demonstrate the effectiveness of the proposed machine design methodology.

REFERENCES

- [1] Changliang Xia, Zhiqiang Li, And Tingna Shi. 2009. "A CONTROL STRATEGY FOR FOUR-SWITCH THREE-PHASE BRUSHLESS DC MOTOR USING SINGLE CURRENT SENSOR". IEEE Trans. Indust. Electron. Vol. 56, No. 6.
- [2] Seok-Myeong Jang, Han-Wook Cho, And Sang-Kyu Choi. 2007. "DESIGN AND ANALYSIS OF A HIGH-SPEED BRUSHLESS DC MOTOR FOR CENTRIFUGAL COMPRESSOR". IEEE Trans. Magnet. Vol. 43, No. 6.
- [3] E. Afjei, H. Toliyat, and H. Moradi. 2006. "A NOVEL HYBRID BRUSHLESS DC MOTOR/GENERATOR FOR HYBRID VEHICLES APPLICATIONS". IEEE PEDES. New Dehli.
- [4] Jang, S.-M., H.-W. Cho, and S.-K. Choi. 2007. "DESIGN AND ANALYSIS OF A HIGH-SPEED BRUSHLESS DC MOTOR FOR CENTRIFUGAL COMPRESSOR". IEEE Trans. Magnet. Vol. 43, No. 6, 2573-2575.
- [5] Taeyong Yoon. 2003. "STATOR DESIGN CONSIDERATION OF A BRUSHLESS DC MOTOR FOR ROBUST ROTOR POSITION DETECTION IN INDUCTIVE SENSE START-UP". IEEE Trans. Magnet. Vol. 42, No. 3.
- [6] Parag R. Upadhyay And K. R. Rajagopal.2006. "FE ANALYSIS AND COMPUTER-AIDED DESIGN OF A SANDWICHED AXIAL-FLUX PERMANENT MAGNET BRUSHLESS DC MOTOR". IEEE Trans. Magnet. Vol. 42, No. 6.
- [7] Miroslav Markovic And Yves Perriard. 2009." OPTIMIZATION DESIGN OF A SEGMENTED HALBACH PERMANENT-MAGNET MOTOR USING AN ANALYTICAL MODEL". IEEE Trans. Magnet. Vol. 45, No. 7.
- [8] Rafal Wrobel And Phil H. Mellor 2008. "DESIGN CONSIDERATIONS OF A DIRECT DRIVE BRUSHLESS MACHINE WITH CONCENTRATED WINDINGS". IEEE Trans. Energy Convers. Vol. 23, No. 1.
- [9] Zhuoran Zhang, Yangguang Yan, Shanshui Yang, And Zhou Bo. 2009. "DEVELOPMENT OF A NEW PERMANENT-MAGNET BLDC GENERATOR USING 12-PHASE HALF-WAVE RECTIFIER". IEEE Trans. Indust. Electron. Vol. 56, No. 6.
- [10] Pan Seok Shin, Han-Deul Kim And Gyo-Bum Chung. 2007. "SHAPE OPTIMIZATION OF A LARGE-SCALE BLDC MOTOR USING AN ADAPTIVE RSM UTILIZING DESIGN SENSITIVITY ANALYSIS". IEEE Trans. Magnet. Vol. 43, No. 4.
- [11] Pan Seok Shin, Sung Hyun Woo, And Chang Seop Koh. 2009. "AN OPTIMAL DESIGN OF LARGE SCALE PERMANENT MAGNET POLE SHAPE USING ADAPTIVE RESPONSE SURFACE METHOD WITH LATIN HYPERCUBE SAMPLING STRATEGY". IEEE Trans. Magnet. Vol. 45, No. 3.
- [12] Rabinovici, R. 1996. "MAGNETIC FIELD ANALYSIS OF PERMANENT MAGNET MOTORS".. IEEE Trans. Magnet. Vol. 32, No. 1, 265- 269.
- [13] Infolytica Corporation Ltd. 2007. Magnet CAD package: User manual. Montreal, Canada: Infolytica.
- [14] Wang, X. H., Q. F. Li, and S. H. Wang. 2003. "ANALYTICAL CALCULATION OF AIR-GAP MAGNETIC FIELD DISTRIBUTION AND INSTANTANEOUS

CHARACTERISTICS OF BRUSHLESS DC MOTORS". IEEE Trans. Energy Convers. Vol. 18, No. 3, 424-432.

[15] J. P. Webb. 2008. "SINGULAR TETRAHEDRAL FINITE ELEMENTS OF HIGH ORDER FOR SCALAR MAGNETIC AND ELECTRIC FIELD PROBLEMS". IEEE TRANS. MAGNET. VOL. 44, NO. 6.

[16] Z. Ren. 2002. "T- Ω FORMULATION FOR EDDY-CURRENT PROBLEMS IN MULTIPLY CONNECTED REGIONS", IEEE TRANS. MAGNET. VOL. 38, NO. 2.

[17]H. Moradi, E. Afjei, And F. Faghihi, "Fem Analysis For A Novel Configuration Of Brushless Dc Motor Without Permanent Magnet", Progress In Electromagnetics Research, Pier 98, 407-423, 2009.